Journal of Physics and Chemistry of Solids 99 (2016) 75–81

Contents lists available at ScienceDirect

Journal of Physics and Chemistry of Solids

journal homepage: www.elsevier.com/locate/jpcs

Exploring the electronic structure of Pb^{2+} ions containing material $Pb_{16}(OH)_{16}(NO_3)_{16}$

A.H. Reshak [a,b,*]

[a] New Technologies - Research Centre, University of West Bohemia, Univerzitni 8, 306 14 Pilsen, Czech Republic
[b] School of Material Engineering, University Malaysia Perlis, 01007 Kangar, Perlis, Malaysia

ARTICLE INFO

Article history:
Received 11 May 2016
Received in revised form
23 July 2016
Accepted 16 August 2016
Available online 17 August 2016

Keywords:
Electronic materials
Inorganic compounds
Semiconductors
Crystal structure
Electronic structure

ABSTRACT

A theoretical band structure calculation for lead nitrate hydroxide $Pb_{16}(OH)_{16}(NO_3)_{16}$ single crystal was performed based on the experimental crystallographic data obtained by Chang et al. Calculations exhibit that the conduction band minimum (CBM) is situated at Γ the center of the Brillouin zone (BZ) while the valence band maximum (VBM) is located between Γ and Y points of the BZ, resulting in an indirect energy band gap of about 3.70 eV in close agreement to the measured one (3.78 eV). The angular momentum resolved projected density of states reveals the existence of the strong hybridization between the orbitals and the VBM is originated from Pb-6s/6p and O-2p orbitals while the CBM from N-2p and Pb-6p orbitals. The calculated valence electronic charge density distribution explore the bond characters and the dominancy of the covalent bonding between Pb–O of PbO_n ployhedra and N–O of $[NO_3]^-$ triangle. The calculated bond lengths and angles show good agreement with the experimental data.

© 2016 Elsevier Ltd. All rights reserved.

1. Introduction

Borates are the excellent materials as solid state lasers [1–3], polarizer and beam displacers [4], since the crystals can be transparent up to the deep UV region and are highly resistive to laser damage [5–9]. The first principle method has been used to calculate the birefringence values of five lead borates, $Pb_8B_9O_{21}F$, $PbBiBO_4$, Pb_3BO_4F, $Pb_6B_3O_{10}Cl$, and Pb_2BO_3F with network B–O structure or isolated BO_3 groups [10]. The calculations show that $PbBiBO_4$, Pb_3BO_4F, and Pb_2BO_3F have the large birefringence, greater than 0.1. Pb_2BO_3F, especially, is the first compound with large birefringence above 0.08 among positive uniaxial borate crystals. It has been found that the parallel arrangement of fundamental building units is not the only light anisotropy active character. In the further research of Pb_2BO_3F, polarization disproportionation via a visualized model is first put forward for identifying the origin of large birefringence, which will be helpful to search for new optical materials with suitable birefringence. Li et al. [11] have investigated the electronic structures and optical properties of a class of lead borates $Pb_2B_5O_9Cl$, $BaPb[B_5O_9(OH)]\cdot H_2O$, and $Ba_2Pb(B_3O_6)_2$ to uncover the influence of the lead atom on the band gap and hence the resulting properties. It is found that $BaPb[B_5O_9(OH)]\cdot H_2O$ and $Ba_2Pb(B_3O_6)_2$ have little band gap redshift due to their weak distortion and stereochemical activity. The intensity of the lead lone pair stereochemical activity plays an important role in determining the reduction of the band gap. Therefore, similar to BO_3^{3-}, BO_3^{4-} or BO_4^{5-} clusters the NO_3^-clusters can be the sources of strong microscopic properties. Several research groups were investigated the properties of NO_3^- containing materials [12]. Recently, a novel promising lead nitrate hydroxide $Pb_{16}(OH)_{16}(NO_3)_{16}$ single crystal has been synthesized using hydrothermal method [13]. It has been found that the novel single crystal is build from $[Pb_4(OH)_4]^{4+}$ cubanes and nitrate form the overall three-dimensional structure via weak Pb–O bonds [13]. The single crystal x-ray diffraction reveals that lead nitrate hydroxide $Pb_{16}(OH)_{16}(NO_3)_{16}$ crystallizes in monoclinic space group (Cc) with four formula per unit cell [13]. The reported unit cell dimensions are $a=25.4814(12)$ Å, $b=17.1832(8)$ Å, $c=18.1746(9)$ Å, $\beta=133.54°$ and $Z=4$ [13]. It is very interesting to highlight that Grimes et al. [14] has been determined the crystal structure of $[Pb_4(OH)_4][NO_3]_4$ by single-crystal x-ray diffraction and refined by full-matrix least-squares analysis with different space group (Ia) and lattice parameters $a=18.251(5)$, $b=17.206(5)$, $c=18.588(12)$Å, $\beta=91.90(4)°$ and $Z=16$. The R values (R1 = 0.076; wR2 = 0.183) found to be high. Therefore, Chang et al. [13] performed better refinements to gain R1 less than 0.05. Developing high efficient nonlinear optical (NLO) crystals for ultra-violet (UV) and deep-UV applications is important for laser spectroscopy, laser processing, including laser-tailoring of molecules, optical triggering and efficient photonic devices [1,15–24]. Chang et al. reported that the $Pb_{16}(OH)_{16}(NO_3)_{16}$ single crystal is type I phase-matchable crystal

* Correspondence address: New Technologies - Research Centre, University of West Bohemia, Univerzitni 8, 306 14 Pilsen, Czech Republic.
E-mail address: maalidph@yahoo.co.uk

http://dx.doi.org/10.1016/j.jpcs.2016.08.011
0022-3697/© 2016 Elsevier Ltd. All rights reserved.

and the local dipole moment of PbO_n polyhedra is larger than that of NO_3^- triangles. Therefore, based on Chang et al. investigation we have performed comprehensive density functional calculations to investigate the electronic structure, total and partial density of states, the valence electronic charge density distribution and the chemical bonding characters. Calculations were performed using the all-electron-full-potential method within two exchange and correlation (XC) potentials so as to ascertain the influence of the XC potentials on the electronic band structure, energy band gap and hence the resulting properties. The previous report [13] performed a theoretical calculations using non-full potential method within the generalized gradient approximation (GGA). It is well known that GGA underestimated the energy band gap value and hence the obtained results. Therefore, for more accurate results we have addressed ourselves to perform comprehensive full potential calculations within the recently modified Becke–Johnson potential (mBJ). The first-principles calculation has proven to be a powerful and useful tool to predict the crystal structure and its properties which are related to the electron configuration of a material before its synthesis [25–27].

2. Methodology

Based on the density functional theory (DFT) within the all-electron full-potential linearized augmented plane wave plus local orbitals (FP-LAPW+lo) method as implemented in WIEN2k package [28], a comprehensive theoretical calculation was performed to calculate the electronic properties of lead nitrate hydroxide $Pb_{16}(OH)_{16}(NO_3)_{16}$. The crystallographic data reported by Chang et al. [13] was used as input to perform the geometrical relaxation by minimizing the forces acting on each atom. The relaxation was achieved by using Perdew–Burke–Ernzerhof generalized gradient approximation (PBE-GGA) [29]. The relaxed geometrical parameters in comparison with the experimental data [13] were listed in Table S1- Supplementary materials. From the relaxed geometry the electronic band structure was obtained using PBE-GGA and the recently modified Becke–Johnson potential (mBJ) [30] as shown in Fig. 1. After details comparison between the two exchange-correlation potentials (see Figs. S2 and S3 - supplementary materials) we found that mBJ succeed by large amount in bringing the calculated energy gap closer to the experimental one. Therefore, we select to show only the results obtained by mBJ. Based on the calculated band structure the total and partial density of states (DOS) were calculated by means of the modified tetrahedron method [31]. The input required for calculating the DOS are the energy eigenvalues and eigenfunctions which are the natural outputs of a band structure calculation. The total DOS and partial DOS are calculated for a large energy range (− 10.0 eV up to 15.0 eV). The states below the Fermi energy (E_F) are the valence states and states above E_F are the conduction states. Hence we obtain DOS for both valence and conduction band states. The lead nitrate hydroxide $Pb_{16}(OH)_{16}(NO_3)_{16}$ crystallizes in monoclinic space group with four formulas per unit cell [13]. The unit cell consist of 112 atoms, 16 Pb atom, 16 nitrates, 16 hydrogen and 64 oxygen atoms. Each N atom connected to three oxygen atoms to form the $[NO_3]^-$ triangle the other oxygen atoms were connected to Pb atoms to form the PbO_n ploydedra. The unit cell is illustrated in Fig. 2.

To insure that there is no charge leakage out of the atomic sphere cores we have used the minimum radius of the muffin-tin spheres (R_{MT}) values as 2.24 a.u. for Pb atoms, 1.03 a.u. for N atoms, 1.08 a.u. for O atoms and 0.59 for H atoms. The R_{MT}'s were chosen in such a way that the spheres did not overlap. The basis functions inside the interstitial region were expanded up to $R_{MT} \times K_{max} = 7.0$ and inside the atomic spheres for the wave function, in order to achieve the total energy convergence. The potential for the construction of basis functions inside the sphere of the muffin-tin was

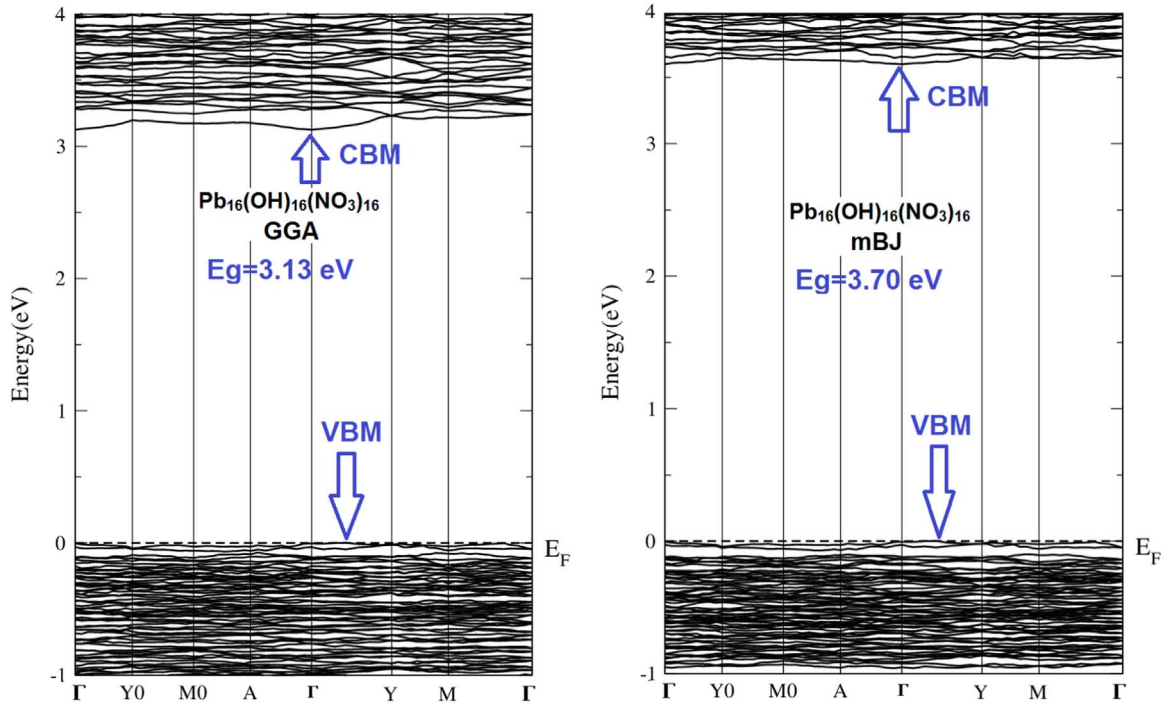

Fig. 1. (Left panel) the calculated The calculated band structure of $Pb_{16}(OH)_{16}(NO_3)_{16}$ using PBE-GGA which show that the energy band gap of about 3.13 eV; (Right panel) The calculated band structure of $Pb_{16}(OH)_{16}(NO_3)_{16}$ using mBJ which show that the energy band gap of about 3.70 eV. Calculations exhibit that the conduction band minimum (CBM) is situated at the center (Γ) of the Brillouin zone (BZ) while the valence band maximum (VBM) is located between Γ and Y points of the BZ, resulting in an indirect energy band gap.

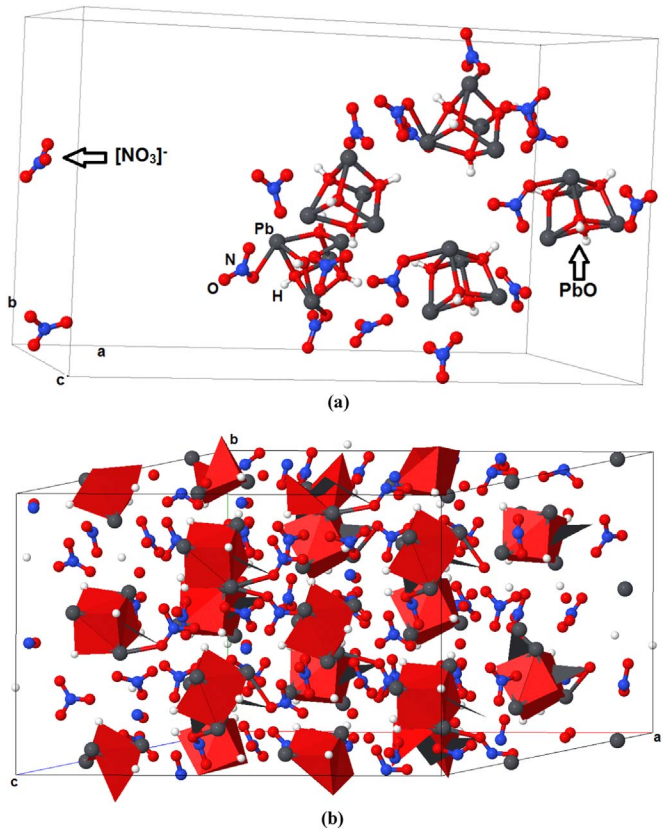

Fig. 2. Crystal structure of led nitrate hydroxide $Pb_{16}(OH)_{16}(NO_3)_{16}$ single crystal. The crystal is formed by $[Pb_4(OH)_4]^{4+}$ cubanes and nitrate form the overall three-dimensional structure via weak Pb–O bonds. The $[Pb_4(OH)_4]^{4+}$ cubanes formed by four Pb atoms and for OH^-. The figure shows the PbO_n polyhedra and NO_3^- triangles. The OH groups are situated above the faces of the Pb_4 tetrahedron giving each Pb atom a trigonal-pyramidal arrangement of nearest-neighbor oxygen atoms in which each Pb atom linked to three OH^-.

spherically symmetric, whereas outside the sphere it was constant [32]. The maximum value of $\boldsymbol{l}$ were taken as $\boldsymbol{l}_{max}=10$, while the charge density is Fourier expanded up to G_{max} = 12.0 $(a.u)^{-1}$. A self-consistency is obtained using 300 $\vec{k}$ points in the irreducible Brillouin zone (*IBZ*). Since the total energy of the system is stable within 0.00001 Ry therefore, the self-consistent calculations are converged. The electronic band structures calculation, density of states and the electronic charge density are performed within 1000 $\vec{k}$ points in the *IBZ*. Our tests reveal that the above-mentioned computational parameters are sufficiently accurate for the present calculations.

3. Results and discussion

From the relaxed geometry of $Pb_{16}(OH)_{16}(NO_3)_{16}$ the electronic band structure was calculated. The electronic band structure give a clear map of the bands dispersion along the high symmetry points of the first BZ. It is interesting to show the conduction and the valence bands dispersion around Fermi level (E_F) to gain clear visualization for the nature of the energy band gap and the orbitals which form these bands. It has been found that the conduction band minimum (CBM) is situated at the center of the Brillouin zone (Γ) while the valence band maximum (VBM) is located between Γ and Y points of the BZ, resulting in an indirect energy band gap of about 3.13 eV (PBE-GGA) and 3.70 eV (mBJ) as shown in Fig. 1. The later show close agreement with the measured one (3.78 eV) [13] and much better than the previous calculated gap (2.779 eV) using CASTEP code within GGA [13] (see Fig. S1-Supplementry materials). We set the zero-point of energy (Fermi level) at VBM. The electronic structure show that the B−O anionic groups are the main factor to influence band gap and hence the related properties [10]. As the unit cell of lead nitrate hydroxide $Pb_{16}(OH)_{16}(NO_3)_{16}$ consist of 112 atoms with four formulas per unit cell thus, the dispersion of the band structure is very congested therefore, we chose to show the bands dispersion around E_F between −1.0 eV and 4.0 eV (Fig. 1). Further, the total density of states (TDOS) and the angular momentum resolved projected density of states (PDOS) using PBE-GGA, mBJ and mBJ with spin-orbit coupling (mBJ+soc) were obtained from the calculated band structure by means of the modified tetrahedron method (see Fig. 3, Figs. S2 and S3 - Supplementary materials). It has been found that the spin-orbit coupling has a significant influence on the band gap. It has been found that the spin-orbit coupling modifies strongly the CBM and results in a band gap reduction of 0.3 eV, similar to the behavior noticed in Refs. [33 and 34]. This can easily be explained by the fact that spin orbit coupling splits the CBM and VBM resulting in gap reduction. For an indirect gap, the role of the phonons is very important. Since mBJ succeed by large amount in bringing the calculated energy gap closer to the experimental one. Therefore, we select to show the results obtained by mBJ in comparison to that obtained by mBJ+soc as illustrated in Fig. 3(a)–(e) which confirm the band gap's value of about 3.70 eV using mBJ and 3.40 eV using mBJ+soc. Therefore, a material with such an energy band gap value is expected to possess a high laser damage threshold [35,36]. The PDOS enables us to identify the angular momentum characters of the various structures as shown in Fig. 3(f)–(i). It has been noticed that the VBM is mainly formed by Pb-6s, O-2p, Pb-6p orbitals with small contribution from Pb-5d/4f orbitals while the CBM is mainly formed by N-2p and Pb-6p orbitals with small contribution of N-2s and O-2s orbitals. The O-2s/2p states are belong to $[OH]^-$ and $[NO_3]^-$ triangle groups. The calculated partial DOS for the energy range (−10.0 eV up to 15.0 eV) are shown in Fig. 3(b)–(e). The structure between −9.0 and −6.0 eV is mainly formed by N-2p, Pb-6s, O-2p, H-1s states with small contribution from Pb-6p state. The second structure from −6.0 eV up to E_F is mainly constructed by O-2p and Pb-6s states with small contribution from Pb-6p/5d, H-1s and O-2s states. The structure from CBM and above is formed by N-2p, Pb-6p, O-2p states with mixture of N-2s, O-2s, Pb-5d/4f and H-1s states. It has been found that there exists a strong hybridization below E_F between O-2p and Pb-6s states, and N-2p hybridized with O-2p and Pb-6s, whereas above E_F the N-2p state hybridized with O-2p state, O-2s with Pb-5d state while Pb-4f hybridized with N-2s and O-2s states. The degree of the hybridization depends on the electronegativity differences between the atoms. According to Pauling scale the electronegativity of Pb, N, O and H are 2.33, 3.04, 3.44 and 2.20, respectively. It is clear that the electronegativity difference between the atoms is small indicating the strong hybridization between the atoms as it clear from Fig. 3(b). This indicate the presence of the covalent bonding, the strength of the covalent bonding depend on the degree of the hybridization. To investigate this, a deep visualization can be gained from the valence electronic charge density distribution (VECD). Therefore, we have calculated the VECD in two different crystallographic planes. These are (1 0 0) and (1 0 1) as shown in Fig. 4(a) and (b). The contour plots reveals that there exists a strong covalent bonding between O and N atoms (electronegativity difference is 0.40) and O atom form a covalent bond with Pb atom (electronegativity difference is 1.11). Due to the high electronegativity for O and N atoms therefore, a charge transfer

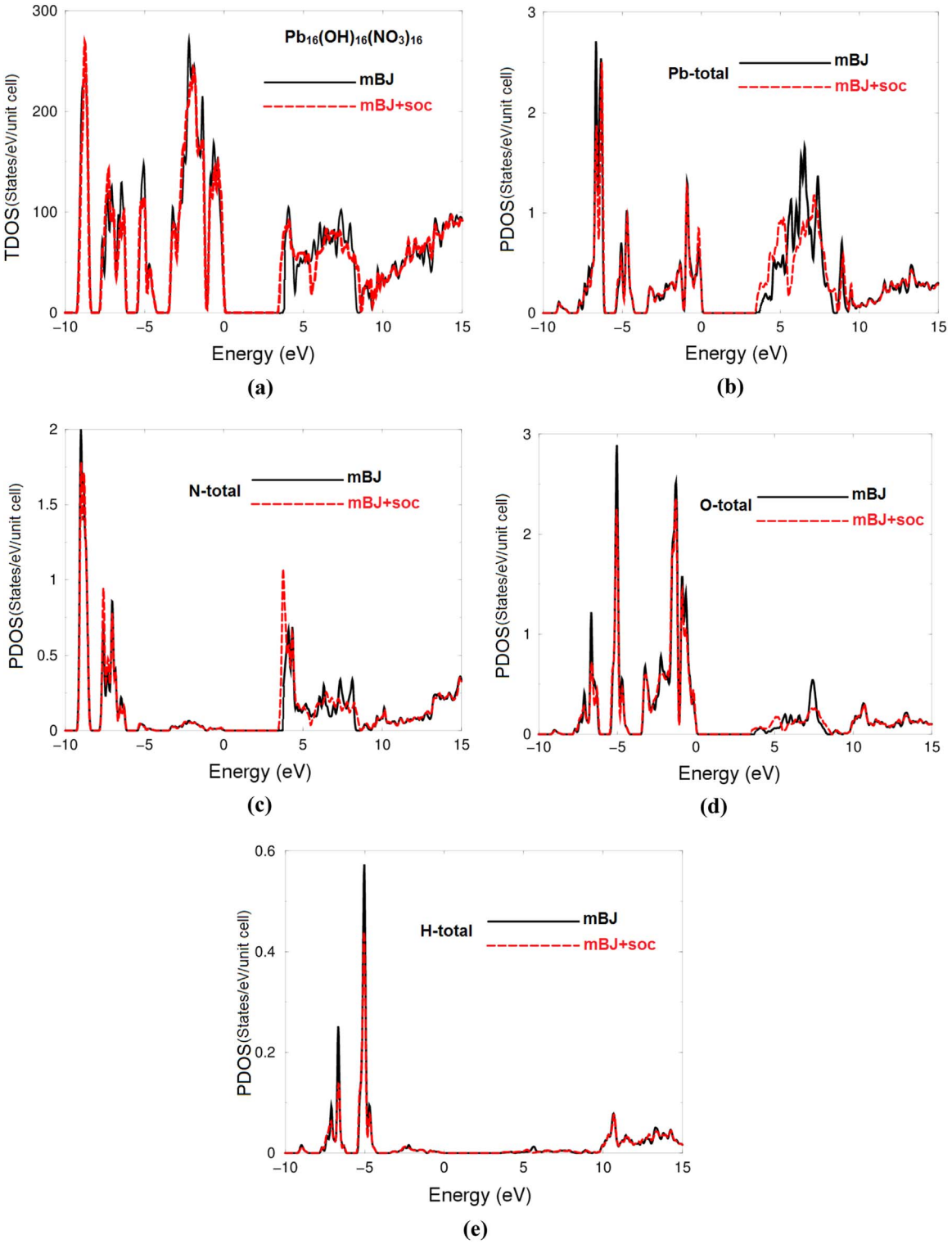

Fig. 3. Calculate total and partial density of states of led nitrate hydroxide $Pb_{16}(OH)_{16}(NO_3)_{16}$ single crystal; (a) calculated total density of states using mBJ and mBJ+soc; (b) calculated total density of states for Pb atoms using mBJ and mBJ+soc; (c) calculated total density of states for N atoms using mBJ and mBJ+soc; (d) calculated total density of states for O atoms using mBJ and mBJ+soc; (e) calculated total density of states for H atoms using mBJ and mBJ+soc; (f) calculated total density of states for Pb, N, O atoms using mBJ; (g) calculated total density of states for H atoms and H-s state using mBJ; (h) calculated partial density of states for Pb-s/p, N-p and O-p states using mBJ; (i) calculated partial density of states for Pb-d/f, N-s and O-s states using mBJ.

occurs towards O and N atoms as indicated by the blue color surrounding both O and N atoms. According to the thermo-scale (Fig. 4) the blue color refer to the maximum charge while the red color indicating the zero charge. We should emphasize that the covalent bonding is more favorable for the transport of the carriers than ionic one [37]. The contour plot exhibit that each N atom connected to three oxygen atoms to form the $[NO_3]^-$ triangle and the other oxygen atoms were connected to Pb atoms to form the PbO_n ployhedra (see Fig. 4(a) and (b)). Also it can be seen that each two neighbors of the PbO_n ployhedra are oriented to the same

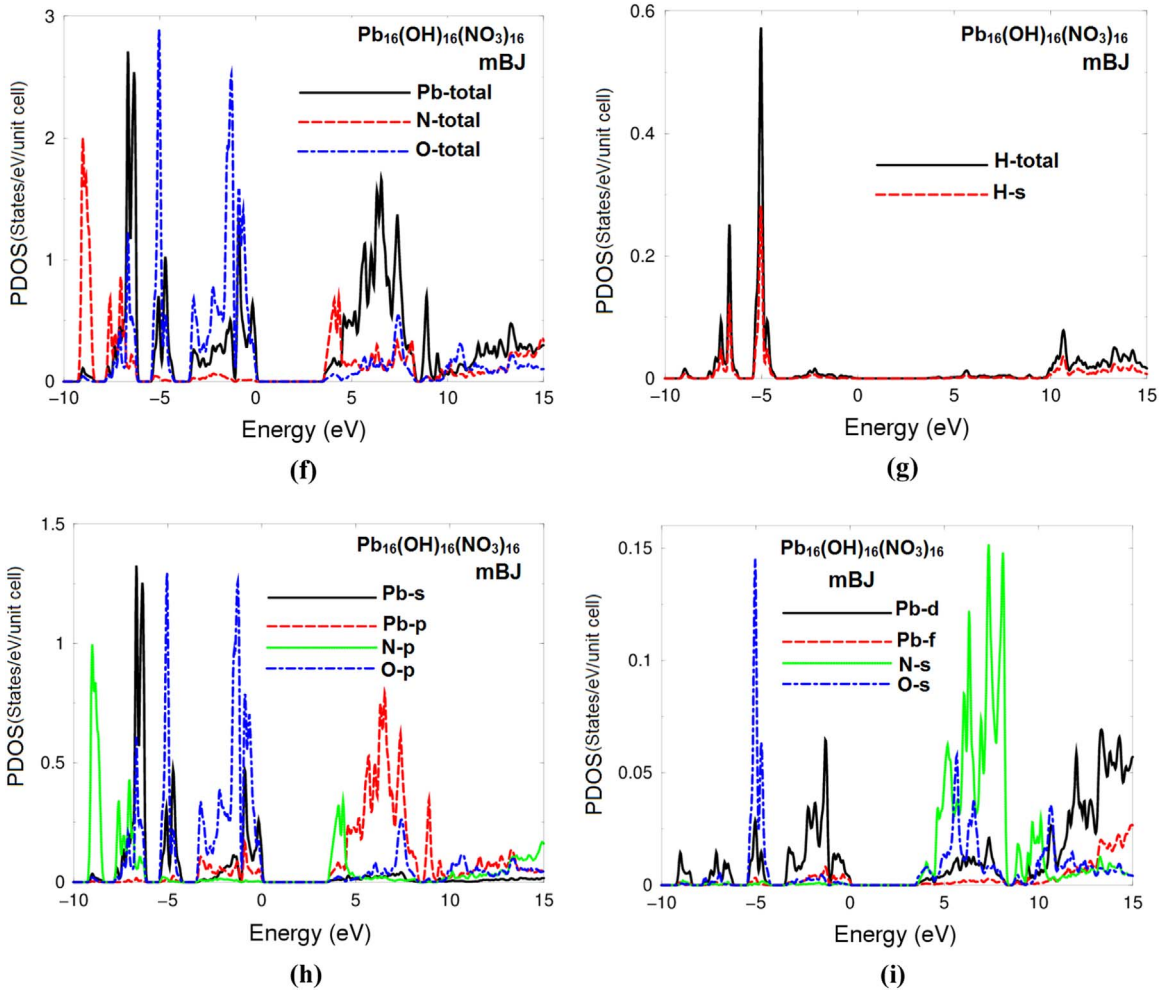

Fig. 3. (*continued*)

directions while the $[NO_3]^-$ are almost randomly oriented (see Fig. 2(a)). The electron cloud of the NO_3 anionic groups exhibit planar shape with conjugated electron orbitals (see Fig. 4(a) and (b)). Also the contour plot reveals that the 6 s^2 lone pair on Pb^{2+} cation posses spherical shape (see Fig. 4(a) and (b)) therefore, the Pb^{2+} cation has an inert or non-stereoactive lone pair. Because of the lone electron pairs presence, the electron density cloud in Pb ions exhibits low symmetry and produces a certain optical anisotropy [10]. Owing to the repulsion interactions of the lone pairs of Pb^{2+} cations, the Pb^{2+} cations may also lead to a little contribution to the anisotropy. To our best knowledge, investigation into the contribution of heavy metal cations with lone pairs and N−O anionic groups for the structure anisotropy still remains reclusive. The arrangement of heavy atoms and the boron group have significant influences on the structure anisotropy. In addition, the bond lengths and angles of lead nitrate hydroxide $Pb_{16}(OH)_{16}(NO_3)_{16}$ single crystal were calculated and compared with the experimental data [13] as listed in Tables S2 and S3-Supplementry materials. Good agreement was found. The full understanding of the structure property relationships and physical mechanism in $Pb_{16}(OH)_{16}(NO_3)_{16}$ would have great meaning in designing and searching for new optical materials with suitable birefringence [10].

4. Conclusions

An all-electron full-potential calculations within generalized gradient approximation (PBE-GGA) and the recently modified Becke–Johnson potential (mBJ) potentials were used to perform comprehensive theoretical calculations for the novel lead nitrate hydroxide $Pb_{16}(OH)_{16}(NO_3)_{16}$ single crystal. Using PBE-GGA, the experimental crystallographic data was optimized. Calculation reveals that $Pb_{16}(OH)_{16}(NO_3)_{16}$ single crystal posses an indirect energy band gap of about 3.13 eV (PBE-GGA), 3.70 eV (mBJ) and 3.40 eV (mBJ+soc). The spin-orbit coupling modifies strongly the CBM and results in a band gap reduction of 0.3 eV. The mBJ potential brings the calculated energy band gap very close to the measured one. The energy gap value confirms that the $Pb_{16}(OH)_{16}(NO_3)_{16}$ single crystal exhibits an exceptional laser damage threshold and as high efficient NLO crystals for UV and deep-UV applications. The angular momentum resolved projected density of states explore the strong hybridization between the orbitals and reveals the existence of the covalent bonding between Pb–O of PbO_n ployhedra and N–O of

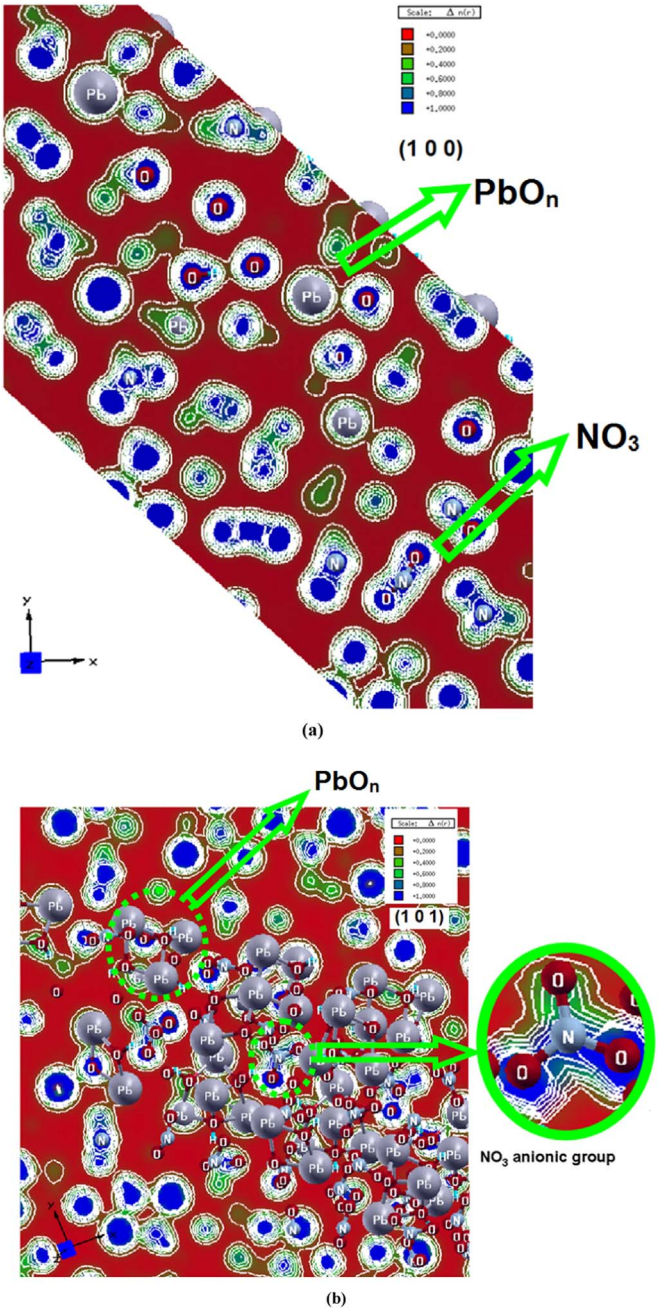

Fig. 4. The calculated electronic charge density distribution in the; (a) (1 0 0) and (b) (1 0 1) crystallographic planes of led nitrate hydroxide $Pb_{16}(OH)_{16}(NO_3)_{16}$ single crystal which shows the PbO_n polyhedra and NO_3^- triangles. The OH groups are situated above the faces of the Pb_4 tetrahedron giving each Pb atom a trigonal-pyramidal arrangement of nearest-neighbor oxygen atoms. The electron cloud of the NO_3 anionic groups which exhibit planar shape with conjugated electron orbitals which make the NO_3 anionic groups are the main source of the large birefringence in $Pb_{16}(OH)_{16}(NO_3)_{16}$.

$[NO_3]^-$ triangle, which confirmed by the calculated valence electronic charge density distribution. The calculated bond lengths and angles show good agreement with the experimental data.

Acknowledgments

The result was developed within the CENTEM project, reg. no. CZ.1.05/2.1.00/03.0088, cofunded by the ERDF as part of the Ministry of Education, Youth and Sports OP RDI programme and, in the follow-up sustainability stage, supported through CENTEM PLUS (LO1402) by financial means from the Ministry of Education, Youth and Sports under the "National Sustainability Programme I. Computational resources were provided by MetaCentrum (LM2010005) and CERIT-SC (CZ.1.05/3.2.00/08.0144) infrastructures.

Appendix A. Supplementary material

Supplementary data associated with this article can be found in the online version at http://dx.doi.org/10.1016/j.jpcs.2016.08.011.

References

[1] Y. Mori, I. Kuroda, S. Nakajima, T. Sasaki, S. Nakai, New nonlinear optical crystal: cesium lithium borate, Appl. Phys. Lett. 67 (13) (1995) 1818–1820.
[2] D. Jaque, O. Enguita, J. Garcı a Sole, A.D. Jiang, Z.D. Luo, Infrared continuous-wave laser gain in neodymium aluminum borate: a promising candidate for microchip diode-pumped solid state lasers, Appl. Phys. Lett. 76 (2000) 2176–2178.
[3] H.W. Yu, H.P. Wu, S.L. Pan, Z.H. Yang, X.L. Hou, X. Su, Q. Jing, K.R. Poeppelmeier, J.M. Rondinelli, Cs3Zn6B9O21: a chemically benign member of the KBBF family exhibiting the largest second harmonic generation response, J. Am. Chem. Soc. 136 (2014) 1264–1267.
[4] R.K. Li, Y.Y. Ma, Chemical engineering of a birefringent crystal transparent in the deep UV range, CrystEngComm 14 (2012) 5421–5424.
[5] M.E. Lines, A.M. Glass, Principles and Applications of Ferroelectrics and Related Materials, Oxford University Press, Oxford 1991, p. 576.
[6] P. Becker, Borate materials in nonlinear optics, Adv. Mater. 10 (1998) 979–992.
[7] Y. Mori, I. Kuroda, S. Nakajima, T. Sasaki, S. Nakai, New nonlinear optical crystal: cesium lithium borate, Appl. Phys. Lett. 67 (1995) 1818–1820.
[8] C.T. Chen, B.C. Wu, A.D. Jiang, G.M. You, A new-type ultraviolet SHG crystal β-BaB2O4, Sci. Sin. Ser. B 28 (1985) 235–243.
[9] K.M. Ok, E.O. Chi, P.S. Halasyamani, Bulk characterization methods for non-centrosymmetric materials: second harmonic generation, piezoelectricity, pyroelectricity, and ferroelectricity, Chem. Soc. Rev. 35 (2006) 710–717.
[10] Q. Bian, Z. Yang, L. Dong, S. Pan, H. Zhang, H. Wu, H. Yu, W. Zhao, Qun Jing, First principle assisted prediction of the birefringence values of functional inorganic borate materials, J. Phys. Chem. C 118 (44) (2014) 25651–25657.
[11] D. Li, Q. Jing, C. Lei, S. Pan, B. Zhang, Z. Yang, Theoretical perspective of the lone pair activity influence on band gap and SHG response of lead borates, RSC Adv. 97 (2015) 79882–79887.
[12] W.T. Dong, H.J. Zhang, Q. Su, Y.H. Lin, S.M. Wang, C.S. Zhu, Crystal growth, structure, and properties of new nonlinear optical materials: K2Ln(NO3) 5 · 2H2O (Ln=La, Ce, Pr, Nd, Sm), J. Solid State Chem. 148 (1999) 302–307.
[13] Lixian Chang, Li Wang, Xin Su, Shilie Pan, Reshalaiti Hailili, Hongwei Yu, Zhihua Yang, A nitrate nonlinear optical crystal Pb16(OH)16(NO3)16 with a large second-harmonic generation response, Inorg. Chem. 53 (2014) 3320–3325.
[14] S.M. Grimes, S.R. Johnston, I. Abrahams, Characterisation of the predominant low-pH lead(II)–hydroxo cation, [Pb4(OH)4]4+; crystal structure of [Pb4(OH)4][NO3]4 and the implications of basic salt formation on the transport of lead in the aqueous environment, J. Chem. Soc. Dalton Trans. 12 (1995) 2081–2086.
[15] C.T. Chen, Y.C. Wu, A.D. Jiang, G.M. You, R. Li, S.L. Lin, New nonlinear-optical crystal LiB3O5, J. Opt. Soc. Am. B 6 (1989) 616–621.
[16] P.S. Halasyamani, K.R. Poeppelmeier, Noncentrosymmetric oxides, Chem. Mater. 10 (1998) 2753–2769.
[17] P.A. Maggard, C.L. Stern, K.R. Poeppelmeier, Understanding the role of helical chains in the formation of noncentrosymmetric solids, J. Am. Chem. Soc. 123 (2001) 7742–7743.
[18] C.F. Sun, C.L. Hu, X. Xu, B.P. Yang, J.G. Mao, Explorations of new second-order nonlinear optical materials in the potassium vanadyl iodate system, J. Am. Chem. Soc. 133 (2011) 5561–5572.
[19] W.L. Zhang, W.D. Chen, H. Zhang, L. Geng, C.S. Lin, Z.Z.J. He, A. Am, Strong second-harmonic generation material Cd4BiO(BO3)3 Originating from 3-chromophore asymmetric structures, Chem. Soc. 132 (2010) 1508–1509.
[20] S.L. Pan, J.P. Smit, B. Watkins, M.R. Marvel, C.L. Stern, K.R. Poeppelmeier, Synthesis, crystal structure, and nonlinear optical properties of Li6CuB4O10: a congruently melting compound with isolated [CuB4O10]6- units, J. Am. Chem. Soc. 128 (2006) 11631–11634.
[21] S.J. Choyke, S.M. Blau, A.A. Larner, S.A. Narducci, J. Yeon, P.S. Halasyamani, A. Norquist, Noncentrosymmetry in new templated gallium fluorophosphates, J. Inorg. Chem. 48 (2009) 11277–11282.
[22] D. Xue, Z. Zhang, Structural analysis of nonlinearities of Ca4ReO.BO3/3(ReDLa, Nd, Sm, Gd, Er, Y), Appl. Phys. A 68 (1999) 57–61.
[23] R.C. Ramachandra, R. Gobinathan, F.D. Gnanan, Growth and characterisation of potassium pentaborate single crystals, Cryst. Res. Technol. 28 (1993), 453; 737.
[24] C. Chen, Y. Wang, Y. Xia, B. Wu, D. Tang, K. Wu, W. Zeng, L. Yu, L. Mei, New development of nonlinear optical crystals for the ultraviolet region with molecular engineering approach, J. Appl. Phys. 77 (1995) 2268.

[25] M. Malachowski, I.R. Kityk, B. Sahraoui, Electronic structure and optical response in $Ga_xAl_{1-x}N$ solid alloys, Phys. Lett. A 242 (1998) 337–342.
[26] I. Fuks-Janczarek, R. Miedzinski, M.G. Brik, A. Majchrowski, L.R. Jaroszewicz, I. V. Kityk, Z-scan analysis and ab initio studies of beta-BaTeMo2O9 single crystal, Solid State Sci. 27 (2014) 30–35.
[27] K.J. Plucinski, I.V. Kityk, J. Kasperczyk, B. Sahraoui, The structure and electronic properties of silicon oxynitride gate dielectrics, Semicond. Sci. Technol. 16 (2001) 467–470.
[28] P. Blaha, K. Schwarz, G.K.H. Madsen, D. Kvasnicka, J. Luitz, WIEN2k, An Augmented Plane Wave Plus Local Orbitals Program for Calculating Crystal Properties, Vienna University of Technology, Austria, 2001.
[29] J.P. Perdew, K. Burke, M. Ernzerhof, Generalized gradient approximation made simple, Phys. Rev. Lett. 77 (1996) 3865–3868.
[30] F. Tran, P. Blaha, Accurate band gaps of semiconductors and insulators with a semilocal exchange-correlation potential, Phys. Rev. Lett. 102 (2009) 226401.
[31] P.E. Blöchl, O. Jepsen, O.K. Andersen, Improved tetrahedron method for Brillouin-zone integrations, Phys. Rev. B 49 (23) (1994) 16223–16233.
[32] K. Schwarz, P. Blaha, Solid state calculations using WIEN2k, Comput. Mater. Sci. 28 (2003) 259.
[33] E. Menendez-Proupin, P. Palacios, P. Wahnon, J.C. Conesa, Self-consistent relativistic band structure of the CH3NH3PbI3 perovskite, Phys. Rev. B 90 (2014) 045207.
[34] Jacky Even, Laurent Pedesseau, Jean-marc Jancu, Claudine Katan, Importance of spin-orbit coupling in hybrid organic/inorganic perovskites for photovoltaic applications, J. Phys. Chem. Lett. 4 (2013) 2999.
[35] J.W. Lekse, M.A. Moreau, K.L. McNerny, J. Yeon, P.S. Halasyamani, J.A. Aitken, Second-harmonic generation and crystal structure of the diamond-like semiconductors Li_2CdGeS_4 and Li_2CdSnS_4, Inorg. Chem. 48 (2009) 7516–7518.
[36] J.A. Brant, D.J. Clark, Y.S. Kim, J.I. Jang, Jian-Han Zhang, J.A. Aitken, Li2CdGeS4, a diamond-like semiconductor with strong second-order optical nonlinearity in the infrared and exceptional laser damage threshold, Chem. Mater. 26 (2014) 3045–3048.
[37] F. Wu, H.Z. Song, J.F. Jia, X. Hu, Prog. Nat. Sci.: Mater. Int. 23 (4) (2013) 408–412.